Direct Integration of Polycrystalline Graphene into Light Emitting Diodes by Plasma-Assisted Metal-Catalyst-Free Synthesis

Yong Seung Kim,[†,‡,¶] Kisu Joo,[§,∥,¶] Sahng-Kyoon Jerng,[†,‡] Jae Hong Lee,[†,‡] Daeyoung Moon,[⊥] Jonghak Kim,[#] Euijoon Yoon,[∥,#] and Seung-Hyun Chun[†,‡,*]

[†]Graphene Research Institute, Sejong University, Seoul 143-747, Korea, [‡]Department of Physics, Sejong University, Seoul 143-747, Korea, [§]Department of Nano Science and Technology, Graduate School of Convergence Science and Technology, Seoul National University, Suwon 443-270, Korea, [∥]Energy Semiconductor Research Center, Advanced Institutes of Convergence Technology, Seoul National University, Suwon 443-270, Korea, [⊥]WCU Hybrid Materials Program, Department of Materials Science and Engineering, Seoul National University, Seoul 151-744, Korea, and [#]Department of Materials Science and Engineering, Seoul National University, Seoul 151-744, Korea. [¶]Y. S. Kim and K. Joo contributed equally to this work.

ABSTRACT

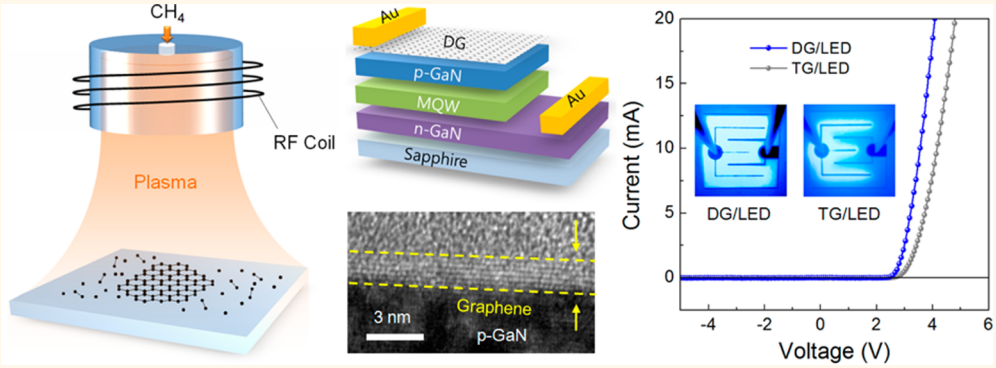

The integration of graphene into devices is a challenging task because the preparation of a graphene-based device usually includes graphene growth on a metal surface at elevated temperatures (~1000 °C) and a complicated postgrowth transfer process of graphene from the metal catalyst. Here we report a direct integration approach for incorporating polycrystalline graphene into light emitting diodes (LEDs) at low temperature by plasma-assisted metal-catalyst-free synthesis. Thermal degradation of the active layer in LEDs is negligible at our growth temperature, and LEDs could be fabricated without a transfer process. Moreover, *in situ* ohmic contact formation is observed between DG and p-GaN resulting from carbon diffusion into the p-GaN surface during the growth process. As a result, the contact resistance is reduced and the electrical properties of directly integrated LEDs outperform those of LEDs with transferred graphene electrodes. This relatively simple method of graphene integration will be easily adoptable in the industrialization of graphene-based devices.

KEYWORDS: graphene · metal-catalyst-free synthesis · plasma-enhanced chemical vapor deposition · light emitting diodes · *in situ* ohmic contact formation

Graphene is an exciting material with a great potential for next-generation electronics and optoelectronics due to its excellent electrical, optical, and mechanical properties.[1−3] Currently, for device applications, large-area graphene films are synthesized by chemical vapor deposition (CVD) at elevated temperatures (~1000 °C) on polycrystalline metal surfaces.[4−6] However, metal catalysts and high growth temperature have hindered the realization of directly integrated graphene devices due to the complicated postgrowth etching/transfer process and the thermal degradation of devices.[6,7] Thus, to achieve direct integration of graphene into devices, graphene has to be synthesized without a metal catalyst at reduced growth temperature.[8] So far, the

* Address correspondence to schun@sejong.ac.kr.

Received for review October 21, 2013 and accepted February 8, 2014.

Published online February 08, 2014
10.1021/nn405477f

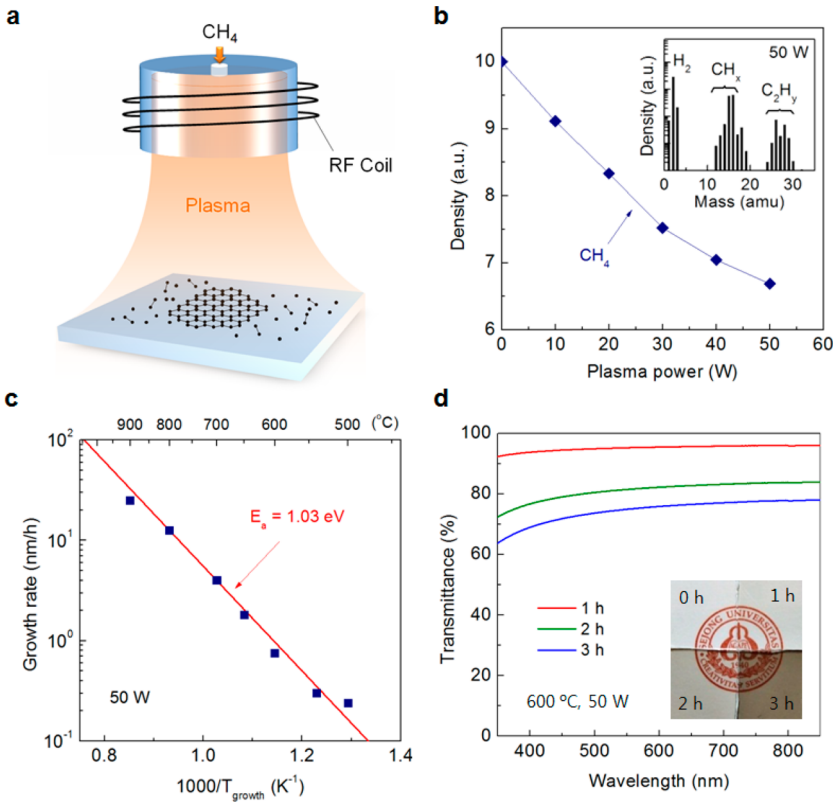

Figure 1. (a) Schematic illustration of the graphene-growth process using the PECVD method. (b) Density variation of methane (CH_4) as a function of plasma power. The inset shows mass spectra of the discharged species measured by a residual gas analyzer at a plasma power of 50 W. (c) Arrhenius plot of the growth rate as a function of the reciprocal substrate temperature. (d) Growth time dependence of optical transmittance of the DG films. The inset shows optical images of DG films grown for different durations.

metal-catalyst-free synthesis of graphene has been tried by thermal CVD (or molecular beam epitaxy) on sapphire,[9−11] quartz,[10,12] SiO_2,[8,12−14] MgO,[15−18] GaN,[19] ZrO_2,[16] Si_3N_4,[20] and HfO_2,[21] which result in graphitic carbon or nanocrystalline graphene. The growth of relatively high quality graphene films on metal-free substrates has been recently demonstrated by several groups. Fanton *et al*. have demonstrated mono- or bilayer graphene growth on sapphire at high temperatures (1425−1600 °C),[22] Bi *et al*. have attempted to grow few-layer graphene on SiO_2 by ambient-pressure CVD at 1100−1200 °C,[23] and Chen *et al*. synthesized high-quality polycrystalline graphene films on Si_3N_4 (1150 °C) and SiO_2 (1100 °C) by employing two-stage and oxygen-aided growth mode, respectively,[24,25] but the high-growth temperature of 1100−1600 °C[22−25] limited its application in optoelectronic devices. Furthermore, considering that ohmic contact is critical for full performance of the devices,[26,27] ohmic contact formation between directly grown graphene (DG) and devices should be required.[19] Therefore, in addition to reducing the growth temperature, finding methods to form ohmic contacts between graphene and a device is imperative to integrate graphene directly into optoelectronic devices.

Here, we demonstrate direct integration of polycrystalline graphene into GaN-based light emitting diodes (LEDs) by PECVD. Due to the advantage of plasma-assisted growth, the growth temperature of graphene is reduced to 600 °C, which is low enough to prevent thermal degradation of active layers in LEDs. This method provides a benefit of *in situ* ohmic-contact formation between graphene and p-GaN, leading to improved performance of LEDs. Electrical properties of directly integrated LEDs outperform those with transferred graphene (TG) electrodes. Further, resulting LEDs exhibit good uniformity in terms of the light output power over 35 LEDs on a centimeter-scale substrate. Our approach, in principle, can be utilized to integrate graphene layers into other substrates or devices.

RESULTS AND DISCUSSION

The growth temperature of graphene on the metal-catalyst-free substrate is reduced by employing PECVD (see Supporting Information Figure S1). Figure 1a presents a schematic illustration of the graphene growth process in a PECVD system. Due to the advantage of plasma-assisted growth, methane is effectively dissociated into various species, such as CH_x, C_2H_y, H, and H_2 (inset of Figure 1b). As shown in Figure 1b, the

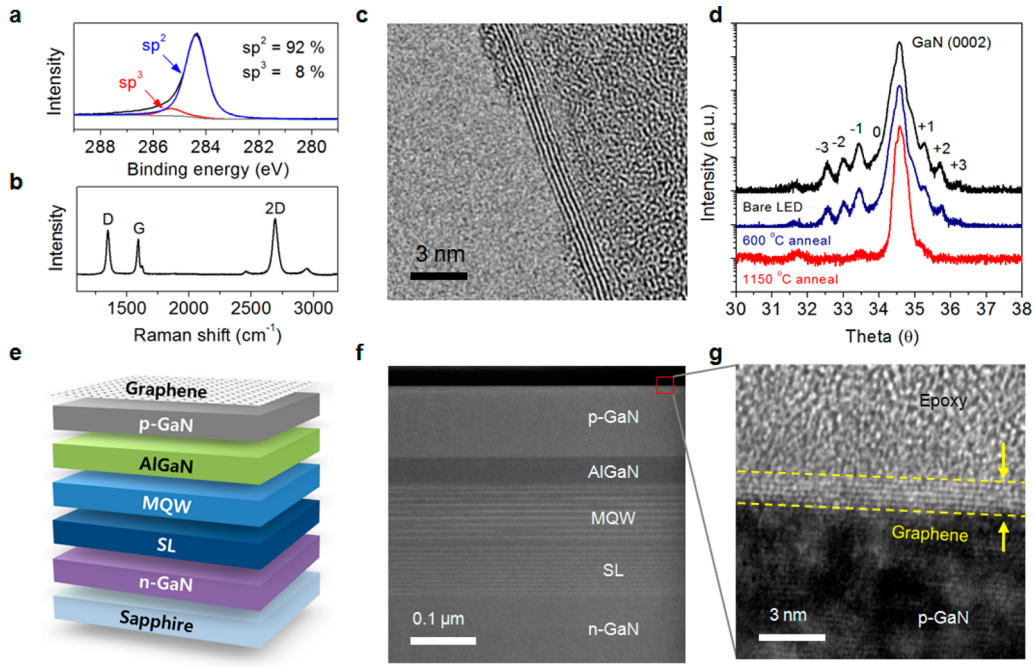

Figure 2. (a) XPS spectra of the C 1s core level and (b) Raman spectra of a DG film synthesized for 3 h under a plasma power of 50 W. (c) HRTEM image of the graphene edge on a TEM grid. (d) HR-XRD curves of the InGaN/GaN MQWs before and after thermal treatment. (e) Schematic diagram and (f) scanning TEM image of the DG/LED structure. (g) HRTEM image at the interface between the p-GaN and DG electrode.

dissociation rate of methane can be tuned by changing the plasma power (see Supporting Information Figure S2 for details of the measurement). When the plasma power is 50 W, the dissociation rate is about 34%, which is significantly higher than that of methane (~0.0002%) in thermal CVD.[28] To investigate the activation energy (E_a) for direct graphene growth in PECVD, we synthesized graphene at various temperatures while the plasma power is fixed at 50 W (see Methods for details of the growth procedure). Figure 1c shows an Arrhenius plot of growth rate *versus* substrate temperature. From the linear fit to the data, E_a was determined to be ~1.03 eV. Considering the higher E_a (2.0−2.6 eV) of graphene growth in thermal CVD,[29,30] this suggests that direct growth of graphene at reduced temperature is enabled by the lowered activation energy resulting from the plasma assistance.

Figure 1d shows the optical properties of synthesized graphene at 600 °C for different durations, investigated by using a double-sided polished sapphire substrate as the reference. The transparencies of graphene films varied depending on the growth duration: ~95%, ~82%, and ~75% at 550 nm when they were grown for 1, 2, and 3 h, respectively (the optical images of these films are presented in the inset of Figure 1d). This result suggests the potential use of DG as window electrodes in LEDs.

The microstructure of DG was probed by X-ray photoelectron spectroscopy (XPS), Raman spectroscopy, high-resolution transmission electron microscopy (HRTEM), and selected-area electron diffraction (SAED). Figure 2a shows C 1s core-level XPS spectrum of the synthesized graphene. The dominating single peak at 284.4 eV (~92%) is the characteristic signal of sp^2-hybridized carbon atoms in graphene.[31,32] Raman spectra of synthesized graphene in Figure 2b show high intensity of the D peak at ~1350 cm^{-1}, indicating the presence of structural disorder, such as domain boundaries and structural defects,[33] but the intense G (~1580 cm^{-1}) and 2D (~2680 cm^{-1}) peaks support the formation of graphene film on the metal-catalyst-free substrates.[34] To further investigate the microstructure of the samples by HRTEM, the continuous graphene film was transferred onto a TEM grid by substrate etching (see Supporting Information Figure S3). The HRTEM image in Figure 2c clearly shows the layered structure of the synthesized graphene. Electron diffraction by the graphene film exhibits hexagonally arranged spot patterns (Supporting Information Figure S3d). This microstructural information of DG film indicates that polycrystalline graphene film is synthesized without the use of a metal catalyst at low temperature by PECVD, which requires a much higher temperature of ~1100 °C in thermal CVD.[24,25]

Thanks to the reduced growth temperature of DG, the thermal degradation of the active layer in LEDs is negligible. Figure 2d shows the XRD spectra of a bare LED and an annealed LED at 600 °C (our growth temperature) and 1150 °C (direct growth temperature in thermal CVD).[24,25] In the case of the bare LED (the black line in Figure 2d), InGaN (0002) satellite peaks are observed up to the third order which are originated

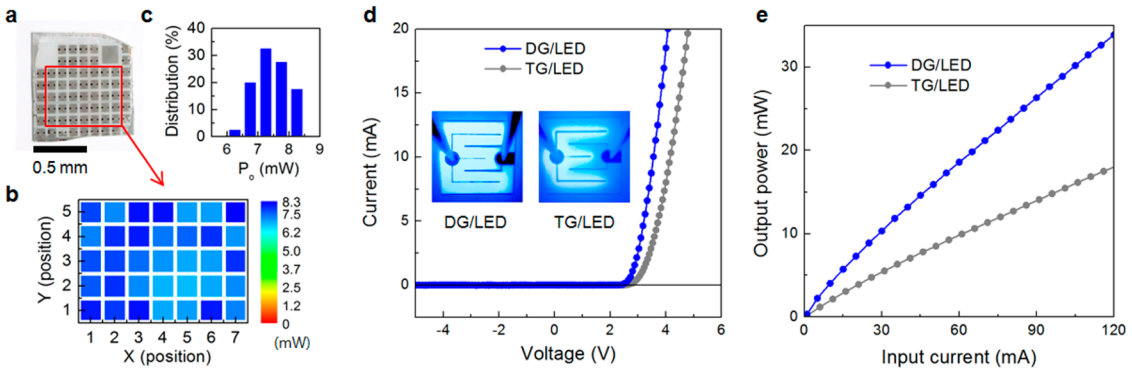

Figure 3. (a) Optical images of the patterned devices on a 1 × 1 cm^2 substrate. (b) Light output power map over 35 DG/LEDs under the input current of 20 mA. (c) Distribution of the light output powers of 35 DG/LEDs. (d) Current−voltage characteristics of LEDs with different electrodes. The insets show optical images of DG/LED (left) and TG/LED (right) after applying an input current of 20 mA. (e) Light output powers of DG/LED and TG/LED as a function of the input current.

from the periodicity of the InGaN/GaN multi-quantum-well (MQW) layers (see schematic diagram of the LED structure in Figure 2e). After annealing at a temperature of 1150 °C, only the zero-order peak is observed (the red line in Figure 2d). The absence of higher-order peaks indicates that the MQW region is replaced by a disordered layer of InGaN through the phase separation of indium in the MQWs.[35,36] However, the XRD spectrum of the LED that was annealed at 600 °C is identical to that of the bare LED spectrum, indicating that the thermal degradation of the MQW layer is negligible at our growth temperature of 600 °C (the blue line in Figure 2d, Supporting Information Figure S4).

The direct growth method of graphene on LEDs enabled the transfer-free approach for the graphene-based transparent conducting electrode. We fabricated GaN-based blue LEDs with DG through a batch process for centimeter-scale LED substrates without a graphene transfer process (see Supporting Information Figure S5 for detailed fabrication procedure). Figure 2e and f show a schematic diagram and a scanning TEM image of LEDs with a DG electrode (DG/LED), respectively. A high-magnification HRTEM image, measured at the interface of the graphene and p-GaN, clearly shows the layered structure of DG on the p-GaN surface (Figure 2g). Additional LEDs with transferred graphene electrodes (TG/LED) are prepared by using graphene films grown on a metal catalyst of Cu foil.[37]

Figure 3a shows an optical image of the DG/LEDs on a 1 × 1 cm^2 wafer. To verify the functionality of DG on the p-GaN layer, the light output power (P_o) of the LEDs was investigated. An output power map of 35 DG/LEDs (marked as red rectangles in Figure 3a) at 20 mA is presented in Figure 3b, showing good uniformity of P_o with mean and standard deviation values of 7.46 mW and 0.46 mW, respectively (Figure 3c). Figure 3d compared the $I-V$ characteristics of DG/LED and TG/LED. In the case of TG/LED, the forward voltage is 4.8 V at 20 mA, which is analogous to the previously reported results for LEDs fabricated with transferred pristine graphene.[38,39] As shown in the right-side inset of Figure 3d, the light emission of TG/LED is not uniform due to incomplete current spreading.[38,40−42] In contrast, the forward voltage of the DG/LED is lowered to 4.1 V at 20 mA. Bright and uniform light emission patterns were observed for the DG/LED (left-side inset of Figure 3d), indicating that the DG electrode works well as a current spreading layer. Moreover, the DG/LED exhibited superior light output power (P_o) in comparison to the TG/LED, as shown in Figure 3e.

Considering the fact that the sheet resistance of DG (∼1.4 kΩ/square; see Methods) is slightly higher than that of TG (∼1.0 kΩ/square), the enhanced electrical performance of DG/LED indicates that there are other important parameters for improved device performances and current spreading for LEDs. One possible reason is plasma-induced damages, such as N loss and point defects, which could act as donor or acceptor levels in GaN,[43] but these defects are not observed in the Raman spectrum of graphene-grown GaN (see Supporting Information Figure S7).[44] We found that plasma-assisted direct integration of graphene on an LED resulted in carbon diffusion into p-GaN and *in situ* ohmic contact formation between graphene and p-GaN. Figure 4a shows secondary ion mass spectrometry (SIMS) profiles of C_{12} intensity for bare and graphene-grown p-GaN substrates, which suggest that carbons are diffused into p-GaN with a depth of 200−300 nm during plasma-assisted graphene growth. The diffused carbon could act as a deep-level acceptor in the form of an interstitial atom or in the complex form with some defects.[25,33,45] To evaluate the DG/p-GaN contact, the current−voltage ($I-V$) characteristics and specific contact resistance (ρ_c) are measured by transmission line method (TLM; see Supporting Information). As shown in Figure 4b, a strong nonlinear behavior is observed in TG/p-GaN, which can be attributed to many factors such as the adhesion and the Schottky barrier between the two layers and the evenness of the graphene surface in contact with the GaN.[40] On the contrary, a linear $I-V$ curve is observed in DG/p-GaN, showing ohmic

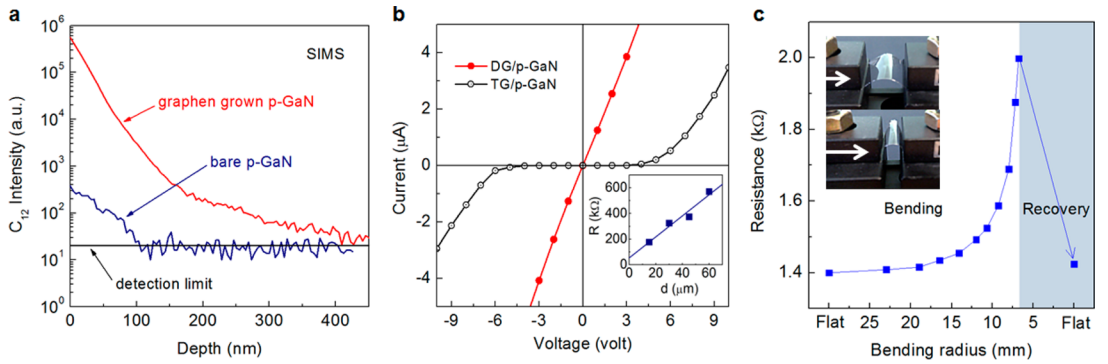

Figure 4. (a) SIMS profiles of C_{12} intensity for virgin and graphene-grown p-GaN. (b) $I-V$ characteristics of DG/p-GaN and TG/p-GaN contacts. The inset shows gap spacing dependence of resistance for specific contact resistance calculation. (c) Electromechanical properties of a graphene film directly grown on a 40-μm-thick mica substrate under bending. The inset shows the bending process.

behavior even in the low voltage range. Presumably the ohmic contact is established through the increased carrier concentration, which is known to reduce the width of the tunneling barrier, followed by the enhancement of carrier tunneling through the barrier.[27,46,47] A specific contact resistance (ρ_c) of 0.15 Ω cm^2 is estimated from the gap spacing dependence of resistance (the inset of Figure 4b). The calculated ρ_c is comparable to the value of 0.6−5.5 Ω cm^2 reported for a graphene/p-GaN contact tailored with a thin Ni/Au interlayer.[48] These results indicate that ohmic contact formation and reduced contact resistance improved current spreading and performances of DG/LEDs.

In view of the potential for integration into flexible devices, the mechanical durability of DG is another important feature. Although the mechanical durability of transferred graphene is well studied,[4,49,50] that of DG has not been reported yet. We synthesized graphene films on flexible 40-μm-thick mica substrates and evaluated the durability of the DG electrodes by measuring the resistance with respect to the bending radius (the inset of Figure 4c). Figure 4c plots the results of the resistance test as a function of different bending radii. The graphene film withstands a bending radius of 7 mm (corresponding to a tensile strain of ~4.7%) and fully recovers after unbending, which reflects the good mechanical properties of DG; note that the indium tin oxide (ITO, the state-of-the-art material for transparent conducting electrodes) is known to be easily broken under 2−3% strain.[51] This result suggests that the practical application of DG can be further expanded into flexible devices.[52]

CONCLUSION

In summary, we have demonstrated plasma-assisted direct integration of graphene on GaN-based LEDs as a transparent conducing electrode, which act as a good current spreading layer. Our approach provides the ultimate advantage of low-temperature, catalyst-free graphene growth and transfer-free device fabrication in addition to *in situ* ohmic contact formation, which is highly desirable for graphene-based optoelectronics. The technique of direct graphene growth on LEDs can be further utilized to integrate graphene into any arbitrary devices, leading to enhanced performance and large-scale, low-cost processing for mass production.

METHODS

Synthesis of Graphene Film. All the graphene films were grown in a PECVD system. A metal-catalyst-free substrate (GaN-based LED, mica, SiO_2/Si) was mounted on the graphite holder and was heated to the growth temperature at a heating rate of 10 °C/min. The graphene was grown by flowing a mixture of methane (CH_4, 2 sccm) and hydrogen (H_2, 20 sccm) while the pressure was maintained at 10 mTorr (inert gases, such as Ar and N_2, are not added in the mixture). The gas mixtures were discharged at a power of 50 W for a specific growth time. The sample was cooled to room temperature at a cooling rate of 3 °C/s by turning off the heating power.

Characterization of Graphene Film. HRTEM studies were conducted on a JEOL JEM-2100F (operating at 200 kV). XPS measurements were performed using a Kratos X-ray photoelectron spectrometer with a Mg Kα X-ray source. Raman spectra were obtained using a Renishaw inVia system with a 514.5 nm laser. AFM images were collected on a PSIA XEI100 system. For transmittance measurements, we used a Varian Cary 5000 UV/vis/NIR spectrophotometer. SIMS measurements were carried out with a Cameca IMS-6f ion microanalyzer, applying a Cs^+ ion beam. The van der Pauw method is used to estimate the transport properties of DG grown on insulating substrates (SiO_2). The sheet resistance and mobility of DG are obtained as 1.4 kΩ/square and 105 cm^2/(V s), respectively. The relatively high sheet resistance of DG can be attributed to the poor crystallinity of DG compared to that of TG, which is consistent with reported data by other groups.[8,14,22]

Measurement of Electrical and Optical Properties. To fabricate the LEDs, InGaN/GaN epitaxially grown wafers (Galaxiaphotonics, peak wavelength = 450 nm) with different transparent electrodes (TG or DG) were partially etched using an ICP etch system (STS, Multiplex ICP system) at a bias power of 100 W. A mixed gas (Cl_2/BCl_3 = 30:5 sccm) was introduced during the etch process to yield an etch rate of 5 nm/s. Subsequently, an electron beam evaporation method (ULTECH, SEE-7D series) was

used to deposit a Ti/Al/Ti/Au (30/100/30/100 nm) metal layer for the ohmic contact to establish simultaneously n-type GaN and current spreading. The $L-I-V$ characteristics were obtained using a Keithley 2425 source measurement unit and a Newport 1936-C spectroradiometer.

Conflict of Interest: The authors declare no competing financial interest.

Acknowledgment. This research was supported by the Priority Research Centers Program (2012-0005859), the Basic Science Research Program (2012-0007298 and 2012-040278), the Center for Topological Matter in POSTECH (2011-0030786), and the Nanomaterial Technology Development Program (2012M3A7B4049888) through the National Research Foundation of Korea (NRF), funded by the Ministry of Education, Science and Technology (MEST). The work was also supported by the WCU Hybrid Materials Program (R31-2008-000-10075-0) and BK21 Plus Program through the National Research Foundation of Korea, funded by the Ministry of Education, Science and Technology, a grant (2010-P2-10) of the Advanced Institutes of Convergence Technology (AICT), and by the Technology Innovation Program (10035430) funded by the Ministry of Knowledge Economy. The authors thank P. Kim (Columbia University) for helpful comments.

Supporting Information Available: Additional figures and data as described in the text. This material is available free of charge *via* the Internet at http://pubs.acs.org.

REFERENCES AND NOTES

1. Novoselov, K. S.; Geim, A. K.; Morozov, S. V.; Jiang, D.; Zhang, Y.; Dubonos, S. V.; Grigorieva, I. V.; Firsov, A. A. Electric Field Effect in Atomically Thin Carbon Films. *Science* **2004**, *306*, 666–669.
2. Geim, A. K.; Novoselov, K. S. The Rise of Graphene. *Nat. Mater.* **2007**, *6*, 183–191.
3. Kim, P.; Zhang, Y. B.; Tan, Y. W.; Stormer, H. L. Experimental Observation of the Quantum Hall Effect and Berry's Phase in Graphene. *Nature* **2005**, *438*, 201–204.
4. Kim, K. S.; Zhao, Y.; Jang, H.; Lee, S. Y.; Kim, J. M.; Kim, K. S.; Ahn, J. H.; Kim, P.; Choi, J. Y.; Hong, B. H. Large-Scale Pattern Growth of Graphene Films for Stretchable Transparent Electrodes. *Nature* **2009**, *457*, 706–710.
5. Li, X. S.; Cai, W. W.; Colombo, L.; Ruoff, R. S. Evolution of Graphene Growth on Ni and Cu by Carbon Isotope Labeling. *Nano Lett.* **2009**, *9*, 4268–4272.
6. Suk, J. W.; Kitt, A.; Magnuson, C. W.; Hao, Y. F.; Ahmed, S.; An, J. H.; Swan, A. K.; Goldberg, B. B.; Ruoff, R. S. Transfer of CVD-Grown Monolayer Graphene onto Arbitrary Substrates. *ACS Nano* **2011**, *5*, 6916–6924.
7. Li, X. S.; Zhu, Y. W.; Cai, W. W.; Borysiak, M.; Han, B. Y.; Chen, D.; Piner, R. D.; Colombo, L.; Ruoff, R. S. Transfer of Large-Area Graphene Films for High-Performance Transparent Conductive Electrodes. *Nano Lett.* **2009**, *9*, 4359–4363.
8. Medina, H.; Lin, Y.-C.; Jin, C.; Lu, C.-C.; Yeh, C.-H.; Huang, K.-P.; Suenaga, K.; Robertson, J.; Chiu, P.-W. Metal-Free Growth of Nanographene on Silicon Oxides for Transparent Conducting Applications. *Adv. Funct. Mater.* **2012**, *22*, 2123–2128.
9. Miyasaka, Y.; Nakamura, A.; Temmyo, J. Graphite Thin Films Consisting of Nanograins of Multilayer Graphene on Sapphire Substrates Directly Grown by Alcohol Chemical Vapor Deposition. *Jpn. J. Appl. Phys.* **2011**, *50*, 04DH12.
10. Sun, J.; Cole, M. T.; Lindvall, N.; Teo, K. B. K.; Yurgens, A. Noncatalytic Chemical Vapor Deposition of Graphene on High-Temperature Substrates for Transparent Electrodes. *Appl. Phys. Lett.* **2012**, *100*, 022102.
11. Jerng, S. K.; Yu, D. S.; Kim, Y. S.; Ryou, J.; Hong, S.; Kim, C.; Yoon, S.; Efetov, D. K.; Kim, P.; Chun, S. H. Nanocrystalline Graphite Growth on Sapphire by Carbon Molecular Beam Epitaxy. *J. Phys. Chem. C* **2011**, *115*, 4491–4494.
12. Kim, K. B.; Lee, C. M.; Choi, J. Catalyst-Free Direct Growth of Triangular Nano-Graphene on All Substrates. *J. Phys. Chem. C* **2011**, *115*, 14488–14493.
13. Sun, J.; Lindvall, N.; Cole, M. T.; Wang, T.; Booth, T. J.; Boggild, P.; Teo, K. B. K.; Liu, J.; Yurgens, A. Controllable Chemical Vapor Deposition of Large Area Uniform Nanocrystalline Graphene Directly on Silicon Dioxide. *J. Appl. Phys.* **2012**, *111*, 044103.
14. Zhang, L. C.; Shi, Z. W.; Wang, Y.; Yang, R.; Shi, D. X.; Zhang, G. Y. Catalyst-Free Growth of Nanographene Films on Various Substrates. *Nano Res.* **2011**, *4*, 315–321.
15. Rummeli, M. H.; Bachmatiuk, A.; Scott, A.; Borrnert, F.; Warner, J. H.; Hoffman, V.; Lin, J. H.; Cuniberti, G.; Buchner, B. Direct Low-Temperature Nanographene CVD Synthesis over a Dielectric Insulator. *ACS Nano* **2010**, *4*, 4206–4210.
16. Scott, A.; Dianat, A.; Borrnert, F.; Bachmatiuk, A.; Zhang, S. S.; Warner, J. H.; Borowiak-Palen, E.; Knupfer, M.; Buchner, B.; Cuniberti, G.; *et al*. The Catalytic Potential of High-Kappa Dielectrics for Graphene Formation. *Appl. Phys. Lett.* **2011**, *98*, 073110.
17. Gaddam, S.; Bjelkevig, C.; Ge, S. P.; Fukutani, K.; Dowben, P. A.; Kelber, J. A. Direct Graphene Growth on MgO: Origin of the Band Gap. *J. Phys.-Condens. Matter* **2011**, *23*, 072204.
18. Jerng, S.-K.; Lee, J. H.; Yu, D. S.; Kim, Y. S.; Ryou, J.; Hong, S.; Kim, C.; Yoon, S.; Chun, S.-H. Graphitic Carbon Growth on MgO(100) by Molecular Beam Epitaxy. *J. Phys. Chem. C* **2012**, *116*, 7380–7385.
19. Sun, J.; Cole, M. T.; Ahmad, S. A.; Backe, O.; Ive, T.; Loffler, M.; Lindvall, N.; Olsson, E.; Teo, K. B. K.; Johan, L.; *et al*. Direct Chemical Vapor Deposition of Large-Area Carbon Thin Films on Gallium Nitride for Transparent Electrodes: A First Attempt. *Semicond. Manuf., IEEE Trans.* **2012**, *25*, 494–501.
20. Sun, J.; Lindvall, N.; Cole, M. T.; Teo, K. B. K.; Yurgens, A. Large-Area Uniform Graphene-Like Thin Films Grown by Chemical Vapor Deposition Directly on Silicon Nitride. *Appl. Phys. Lett.* **2011**, *98*, 252107.
21. Kidambi, P. R.; Bayer, B. C.; Weatherup, R. S.; Ochs, R.; Ducati, C.; Szabo, D. V.; Hofmann, S. Hafnia Nanoparticles - a Model System for Graphene Growth on a Dielectric. *Phys Status Solidi R* **2011**, *5*, 341–343.
22. Fanton, M. A.; Robinson, J. A.; Puls, C.; Liu, Y.; Hollander, M. J.; Weiland, B. E.; LaBella, M.; Trumbull, K.; Kasarda, R.; Howsare, C.; *et al*. Characterization of Graphene Films and Transistors Grown on Sapphire by Metal-Free Chemical Vapor Deposition. *ACS Nano* **2011**, *5*, 8062–8069.
23. Bi, H.; Sun, S. R.; Huang, F. Q.; Xie, X. M.; Jiang, M. H. Direct Growth of Few-Layer Graphene Films on SiO(2) Substrates and Their Photovoltaic Applications. *J. Mater. Chem.* **2012**, *22*, 411–416.
24. Chen, J. Y.; Wen, Y. G.; Guo, Y. L.; Wu, B.; Huang, L. P.; Xue, Y. Z.; Geng, D. C.; Wang, D.; Yu, G.; Liu, Y. Q. Oxygen-Aided Synthesis of Polycrystalline Graphene on Silicon Dioxide Substrates. *J. Am. Chem. Soc.* **2011**, *133*, 17548–17551.
25. Chen, J.; Guo, Y.; Wen, Y.; Huang, L.; Xue, Y.; Geng, D.; Wu, B.; Luo, B.; Yu, G.; Liu, Y. Two-Stage Metal-Catalyst-Free Growth of High-Quality Polycrystalline Graphene Films on Silicon Nitride Substrates. *Adv. Mater.* **2013**, *25*, 992–997.
26. Pearton, S. J.; Ren, F.; Zhang, A. P.; Lee, K. P. Fabrication and Performance of GaN Electronic Devices. *Mater. Sci. Eng., R* **2000**, *30*, 55–212.
27. Kim, T. J.; Holloway, P. H. Ohmic Contacts to GaAs Epitaxial Layers. *Crit. Rev. Solid State* **1997**, *22*, 239–273.
28. Hash, D. B.; Meyyappan, M. Model Based Comparison of Thermal and Plasma Chemical Vapor Deposition of Carbon Nanotubes. *J. Appl. Phys.* **2003**, *93*, 750–752.
29. Kim, H.; Mattevi, C.; Calvo, M. R.; Oberg, J. C.; Artiglia, L.; Agnoli, S.; Hirjibehedin, C. F.; Chhowalla, M.; Saiz, E. Activation Energy Paths for Graphene Nucleation and Growth on Cu. *ACS Nano* **2012**, *6*, 3614–3623.
30. Loginova, E.; Bartelt, N. C.; Feibelman, P. J.; McCarty, K. F. Evidence for Graphene Growth by C Cluster Attachment. *New J. Phys.* **2008**, *10*, 093026.
31. Nikitin, A.; Naslund, L. A.; Zhang, Z. Y.; Nilsson, A. C-H Bond Formation at the Graphite Surface Studied with Core Level Spectroscopy. *Surf. Sci.* **2008**, *602*, 2575–2580.

32. Peltekis, N.; Kumar, S.; McEvoy, N.; Lee, K.; Weidlich, A.; Duesberg, G. S. The Effect of Downstream Plasma Treatments on Graphene Surfaces. *Carbon* **2012**, *50*, 395–403.
33. Lucchese, M. M.; Stavale, F.; Ferreira, E. H. M.; Vilani, C.; Moutinho, M. V. O.; Capaz, R. B.; Achete, C. A.; Jorio, A. Quantifying Ion-Induced Defects and Raman Relaxation Length in Graphene. *Carbon* **2010**, *48*, 1592–1597.
34. Ferrari, A. C.; Meyer, J. C.; Scardaci, V.; Casiraghi, C.; Lazzeri, M.; Mauri, F.; Piscanec, S.; Jiang, D.; Novoselov, K. S.; Roth, S.; *et al*. Raman Spectrum of Graphene and Graphene Layers. *Phys. Rev. Lett.* **2006**, *97*, 187401.
35. McCluskey, M. D.; Romano, L. T.; Krusor, B. S.; Johnson, N. M.; Suski, T.; Jun, J. Interdiffusion of In and Ga in InGaN Quantum Wells. *Appl. Phys. Lett.* **1998**, *73*, 1281–1283.
36. Kim, J.; Kim, H.; Lee, S. N. Thermal Degradation in InGaN Quantum Wells in Violet and Blue GaN-Based Laser Diodes. *Curr. Appl. Phys.* **2011**, *11*, S167–S170.
37. Kim, Y. S.; Lee, J. H.; Kim, Y. D.; Jerng, S. K.; Joo, K.; Kim, E.; Jung, J.; Yoon, E.; Park, Y. D.; Seo, S.; *et al*. Methane as an Effective Hydrogen Source for Single-Layer Graphene Synthesis on Cu Foil by Plasma Enhanced Chemical Vapor Deposition. *Nanoscale* **2013**, *5*, 1221–1226.
38. Jo, G.; Choe, M.; Cho, C. Y.; Kim, J. H.; Park, W.; Lee, S.; Hong, W. K.; Kim, T. W.; Park, S. J.; Hong, B. H.; *et al*. Large-Scale Patterned Multi-Layer Graphene Films as Transparent Conducting Electrodes for GaN Light-Emitting Diodes. *Nanotechnology* **2010**, *21*, 175201.
39. Kim, B.-J.; Lee, C.; Jung, Y.; Baik, K. H.; Mastro, M. A.; Hite, J. K.; Eddy, C. R., Jr.; Kim, J. Large-Area Transparent Conductive Few-Layer Graphene Electrode in GaN-Based Ultra-Violet Light-Emitting Diodes. *Appl. Phys. Lett.* **2011**, *99*, 143101.
40. Chandramohan, S.; Kang, J. H.; Ryu, B. D.; Yang, J. H.; Kim, S.; Kim, H.; Park, J. B.; Kim, T. Y.; Cho, B. J.; Suh, E. K.; *et al*. Impact of Interlayer Processing Conditions on the Performance of GaN Light-Emitting Diode with Specific NiOx/Graphene Electrode. *ACS Appl. Mater. Interfaces* **2013**, *5*, 958–964.
41. Shim, J. P.; Kim, D.; Choe, M.; Lee, T.; Park, S. J.; Lee, D. S. A Self-Assembled Ag Nanoparticle Agglomeration Process on Graphene for Enhanced Light Output in GaN-Based LEDs. *Nanotechnology* **2012**, *23*, 255201.
42. Chandramohan, S.; Kang, J. H.; Katharria, Y. S.; Han, N.; Beak, Y. S.; Ko, K. B.; Park, J. B.; Kim, H. K.; Suh, E. K.; Hong, C. H. Work-Function-Tuned Multilayer Graphene as Current Spreading Electrode in Blue Light-Emitting Diodes. *Appl. Phys. Lett.* **2012**, *100*, 023502.
43. Choi, H. W.; Chua, S. J.; Kang, X. J. Surface Modification and Ohmic Contact Formation to n and p-Type GaN. *Phys. Status Solidi A* **2001**, *188*, 399–402.
44. Choi, H. W.; Chua, S. J.; Tripathy, S. Morphological and Structural Analyses of Plasma-Induced Damage to n-Type GaN. *J. Appl. Phys.* **2002**, *92*, 4381–4385.
45. Jorio, A.; Lucchese, M. M.; Stavale, F.; Ferreira, E. H. M.; Moutinho, M. V. O.; Capaz, R. B.; Achete, C. A. Raman Study of Ion-Induced Defects in N-Layer Graphene. *J. Phys.-Condens. Matter* **2010**, *22*, 334204.
46. Sze, S. M. *Physics of Semiconductor Devices*, 2nd ed.; Wiley: New York, 1981; p xii.
47. Abernathy, C. R.; Pearton, S. J.; Ren, F.; Hobson, W. S.; Fullowan, T. R.; Katz, A.; Jordan, A. S.; Kovalchick, J. Carbon Doping of III-V-Compounds Grown by MOMBE. *J. Cryst. Growth* **1990**, *105*, 375–382.
48. Lee, J. M.; Jeong, H. Y.; Choi, K. J.; Park, W. I. Metal/Graphene Sheets as p-Type Transparent Conducting Electrodes in GaN Light Emitting Diodes. *Appl. Phys. Lett.* **2011**, *99*, 041115.
49. Bae, S.; Kim, H.; Lee, Y.; Xu, X. F.; Park, J. S.; Zheng, Y.; Balakrishnan, J.; Lei, T.; Kim, H. R.; Song, Y. I.; *et al*. Roll-to-Roll Production of 30-Inch Graphene Films for Transparent Electrodes. *Nat. Nanotechnol.* **2010**, *5*, 574–578.
50. Fu, X. W.; Liao, Z. M.; Zhou, J. X.; Zhou, Y. B.; Wu, H. C.; Zhang, R.; Jing, G. Y.; Xu, J.; Wu, X. S.; Guo, W. L.; *et al*. Strain Dependent Resistance in Chemical Vapor Deposition Grown Graphene. *Appl. Phys. Lett.* **2011**, *99*, 213107.
51. Cairns, D. R.; Witte, R. P.; Sparacin, D. K.; Sachsman, S. M.; Paine, D. C.; Crawford, G. P.; Newton, R. R. Strain-Dependent Electrical Resistance of Tin-Doped Indium Oxide on Polymer Substrates. *Appl. Phys. Lett.* **2000**, *76*, 1425–1427.
52. Lewis, J. Material Challenge for Flexible Organic Devices. *Mater. Today* **2006**, *9*, 38–45.